Hindawi
Journal of Food Processing and Preservation
Volume 2024, Article ID 3248305, 11 pages
https://doi.org/10.1155/2024/3248305

Research Article

Development of Plasma-Activated Water (PAW) System: Molecular Dynamics Simulation and Experimental Study on Almond Aflatoxins

Mohammad Javad Aarabi,[1] **Sajad Rostami**,[1] **Bahram Hosseinzadeh Samani**,[1] **and Firouzeh Nazari**[2]

[1]*Department of Mechanical Engineering of Biosystem, Shahrekord University, Shahrekord, Iran*
[2]*Food and Drug Affairs Iran University of Medical Sciences, Tehran, Iran*

Correspondence should be addressed to Sajad Rostami; rostami.sajad@yahoo.com

Received 10 July 2023; Revised 26 November 2023; Accepted 9 January 2024; Published 19 January 2024

Academic Editor: Milan Vukic

Almonds play a significant role in Iran's economy, and factors that threaten their market, such as aflatoxins, need careful consideration. Plasma-activated water (PAW) is a new method that has antioxidant activity and can eliminate toxins and microbial agents, making it a suitable solution for removing aflatoxins from almonds. In a study, the continuous PAW production system was used to control and remove almond aflatoxins, and molecular dynamics simulation was employed to evaluate the impact of PAW on aflatoxin B1. The study found that reducing the flow rate of plasma-treated water had the greatest effect on reducing aflatoxin concentration, followed by PAW application time, the dose of inoculated toxin, and the air/gas mixture ratio. The use of PAW reduced aflatoxin concentration in almonds by 12% to 56.8%. The simulation results suggested that PAW can affect the structure of aflatoxin B1, change and destroy its activity, and reduce its toxicity. Among the free radicals tested, NO_3^- was found to be the most effective in degrading aflatoxin B1. This study demonstrates the potential of PAW as a method to remove aflatoxins and enhance the safety of almonds.

1. Introduction

As the global population continues to grow, the demand for crops has increased significantly, leading to a significant challenge in agricultural production of improving crop yields [1]. Aflatoxins pose a substantial risk to food safety, impeding the trade of dried fruits, walnuts, almonds, and pistachios. Instances of aflatoxin contamination in almonds have been documented [2], raising concerns given the pivotal economic role of almonds in Iran and Chaharmahal and Bakhtiari Province. Any contamination of almonds could create concerns about their safety, leading to a significant impact on the supply and demand market. Aflatoxin's presence significantly hampers the almond industry's sales and growth. Therefore, it is crucial to thoroughly examine and elucidate the factors that pose a threat to the market for this product. Effective control of aflatoxin contamination is crucial for ensuring the safety of almond consumption and trade.

In recent years, nonthermal plasma technology has gained significant attention for its potential to control pathogens in agriculture [3]. Cold atmospheric plasma (CAP) technology has been in use since the 1970s, and it has gradually been used for a variety of purposes, including seed germination, plant growth, insecticide sterilization, virus inhibition, crop preservation, and pesticide residue degradation, as it is fast-acting, efficient, and pollution-free [4–7]. Research studies have shown that this technology can effectively destroy or remove mycotoxins derived from *Aspergillus flavus fungus* [8, 9].

To increase the flexibility and expand the application of CAP technology, researchers have exposed water to various forms of plasma discharge to generate plasma-activated water (PAW) [10–12]. Compared to traditional CAP treatment

methods, PAW offers greater flexibility and safety, enabling effective CAP treatment and overcoming its limitations [3, 13]. PAW is water-activated through reactions with different reactive species, such as free radicals, ions, and electrons generated and used by CAP [14]. Several recent studies have reported the beneficial antimicrobial effects of PAW [15–17]. The improved quality of PAW is mainly attributed to different reactive oxygen and nitrogen species (RONS), composed of plasma chemical species transported through the plasma-water interface. These reactive species include nitrates (NO_3^-), nitrites (NO_2^-), hydrogen peroxide (H_2O_2), ozone (O_3), hydroperoxyl (HO_2), hydroxyl radicals (OH•), nitric oxide (NO•), superoxide (O_2^-), peroxynitrate ($OONO_2^-$), singlet oxygen ($^1O_2$), and peroxynitrites ($ONOO^-$) [16, 18]. In general, PAW contains reactive chemical species that can act as an alternative approach to address microbiological safety while maintaining or promoting other functional properties of crops [19].

Several studies have demonstrated the acute or chronic effects of exposure to aflatoxins on various organs, such as the skin, liver, heart, and lungs [6]. Liver cancer is one of the most common and fatal effects of aflatoxins. The biosynthesis of aflatoxins is a complex process that involves multiple enzymatic reactions and is influenced by various biotic and abiotic factors, including oxidative stress, growth stage, and temperature [20]. The production and stability of aflatoxins also rely on the physiological condition related to the energy levels within the organism. Therefore, molecular dynamics (MD) can be used to evaluate the impact of PAW on aflatoxins.

MD is a computer simulation technique that analyzes the physical movements of atoms and molecules. During the simulation, atoms and molecules interact for a specific time, providing a view of the system's dynamic "evolution." Typically, the trajectories of atoms and molecules are determined by numerically solving Newton's equations of motion for a system of interacting particles. The forces between particles and their potential energies are often calculated using interatomic potentials or molecular mechanics (MM) force fields. Since molecular systems usually consist of numerous particles, it is impossible to determine the characteristics of such complex systems analytically. Therefore, MD simulation via numerical methods is used to resolve this problem [21]. MD is one of the most accurate simulation methods for simulating complex systems in engineering areas. This method solves systems with thousands of interacting particles using relevant equations, and appropriate conditions are determined through statistical mechanics analysis [22]. Under ideal conditions, simulation is considered a powerful scientific tool whose results are comparable to those obtained from laboratory experiments. This method is particularly valuable when the desired sample is expensive, out of reach, or microscopic [23].

According to past studies, no research is simultaneously experimental and computer-based on water-activated aflatoxins in almonds. Finally, the research is aimed at exploring the practical and in silico impact of almond aflatoxins on plasma-activated water (PAW). The study sought to analyze various PAW parameters affecting aflatoxins and evaluate the influence of specific free radicals within PAW, including nitrate (NO_3^-), hydrogen peroxide (H_2O_2), and singlet oxygen ($^1O_2$), on either inhibiting or transforming the form of aflatoxins, employing molecular dynamics (MD) simulations. The MD simulation was performed in the in silico environment, and the effect of PAW on almond aflatoxins was evaluated under the conditions of MD simulation.

2. Materials and Methods

2.1. PAW System. The properties of plasma are influenced by various factors such as the geometric structure of the plasma production system, electrode shape and placement, applied voltage and frequency, electric current, and inherent and fluid properties of the gas [24]. Plasma jet requires the use of Argon, Hydrogen, Helium, Nitrogen, or a combination of these gases. Air, which is a readily available and inexpensive source, contains oxygen and nitrogen, both of which are effective gases for plasma generation.

The atmospheric pressure cold plasma jet with dielectric barrier discharge method was utilized to generate PAW using CAP technology, along with the system designed by Esmaeili et al. [24]. The designed system applies CAP to continuous flow to produce PAW.

The treatment container gradually affects the inlet water with CAP, and the treated water continuously exits the outlet. The inlet flow to the treatment tank is controlled using a check valve. During testing, the input and output flow are regulated and adjusted until a stable flow rate is achieved, ensuring that water treatment with CAP occurs at the appropriate time without interrupting the flow continuity (Figure 1). PAW is generated using deionized water, different argon/air ratios, and flow rates of 0.5, 1, and 1.5 ml/min for water flow passing through the system. Among the possible states (a gas mixture and a water rate), the concentration of nitrate (NO_3^-), hydrogen peroxide (H_2O_2), and singlet oxygen ($^1O_2$) is measured by titration method and using water analysis kits and is used in MD simulation studies. The experimental data obtained from the laboratory studies regarding PAW's effect on aflatoxins are based on this particular state.

2.2. Evaluation of the Effect of PAW on Aflatoxin Reduction or Removal

2.2.1. Aflatoxin Investigation via HPLC Method. Aflatoxin concentration was measured using the HPLC method, and purification was carried out by immunoaffinity column based on the national standard of Iran No. 6872 [24]. A total of 27 Falcon tubes covered with foil were prepared, and ten almonds were placed in each Falcon tube to evaluate the effect of PAW on the reduction of almond aflatoxins based on the design of an almond inoculation experiment with total aflatoxins. Almonds were selected in such a way that their total weight would be equal to 10 grams (g). By sampler, six Falcons with a dose of 5 ppb, fifteen Falcons with a dose of 10 ppb, and six Falcons with a dose of 15 ppb were inoculated. The level of aflatoxin reduction following PAW treatment was determined using HPLC.

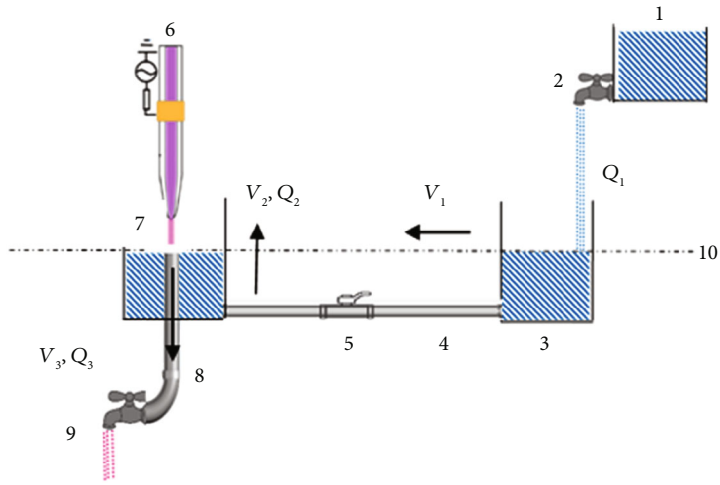

Figure 1: PAW system. (1) Water inlet tank. (2) Inlet flow control valve to the inlet tank to regulate the inlet and generate counter lines between the inlet tank and the treatment tank. (3) Flow inlet tank for flow accumulation and the slow flowing to treatment tank given Pascal's law. (4) Flow connection tube with a diameter of *d*. (5) Flow control valve between two tanks. (6) Dielectric barrier discharge (DBD) plasma set and plasma spray. (7) Treatment tank with a diameter of *D*. (8) Flow outlet tube built in the treatment tank from which the plasma-treated water comes out. (9) Flow outlet control valve. (10) Counter line of two tanks as the boundary flow formation in tube no. 8. Q: water flow rate; V: water flow velocity.

2.2.2. Extraction. The dried almond kernel of the Mamaei variety used in this research was prepared in 2021 from Chaharmahal and Bakhtiari Province, Saman City. A laboratory mill ground the almonds and then sieved them with a 20-mesh sieve. A total of 10 almonds with a total weight of 10 grams (g) were selected. One gram of NaCl, 24 milliliters (ml) of pure methanol, and 20 ml of n-hexane were added to 10 g of paste sample and mixed for 3 minutes in a high-speed laboratory shaker. After separating the n-hexane component from the obtained extract, 24 ml of distilled water was added to 4 ml of the filtered extract. It was then passed through a filter paper. After the immunoaffinity column reached the laboratory temperature, 2 ml PBS buffer was passed through. Next, 14 ml of the diluted extract was passed through the column at one drop per second. In the next stage, the column was rinsed with 15 ml of distilled water and dried using mild-pressure air for 5-10 seconds. Aflatoxins were eluted from the column and collected in a vial, adding 1.5 ml of methanol to the column. Then, 1/5 ml of HPLC-grade water was added to the vial. It was then vortexed and passed through the 45 μm-filter, and 100 microliters (μl) of the solution was injected into the HPLC device.

The standard curve of an aflatoxin mixture with different concentrations was used after quantitatively considering the dilution and recycling coefficient to estimate aflatoxins.

2.2.3. Analysis, Modeling, and Optimization of the Experiment Method. This section determined the optimal conditions for aflatoxin reduction or removal from samples using the response surface method (RSM). RSM is a set of mathematical and statistical techniques utilized for the development, advancement, and optimization of processes in which the given surface is affected by several variables. Using the RSM to establish the relationship between a project's response and independent variables includes the following three steps [25].

Table 1: Levels of selected independent variables in RSM for toxin.

Independent variables	Coding levels		
	-1	0	1
Water rate (ml/min)	0.5	1	1.5
Air/gas mixture ratio (air + argon)	0	0.5	1
PAW application time	1	10	20
Inoculated toxin dose (ppb)	5	10	15

The first step is determining the independent variables, tested surfaces, and type of test plan. The second step is predicting and verifying the accuracy of the model equation, and the third step is obtaining the isoresponse curves and the linear response map as a function of the independent variables. The following equation solution was used to obtain the optimized value [25].

$$Yi = \beta_0 + \sum B_i X_i + \sum \beta_{ii} X_i^2 + \sum \beta_{ii} X_i X_{ij} + \varepsilon, \quad (1)$$

where β_0, β_i, and β_{ii} denote the constant coefficients, X_i and X_{ij} are the independent variables in the process, and ε shows the random error. Considering the available sources, the range of variation of the independent variables in the experiment was selected following Table 1 [25].

3. Molecular Dynamics Simulation and In Silico Study

We use in silico studies to evaluate PAW's effect on aflatoxin's structure. Studies on PAW have shown that its main active substances include reactive oxygen species (ROS) and reactive nitrogen species (RNS) [7]. The main components of ROS include hydroxyl radicals, hydrogen peroxide, singlet

Table 2: Results of *statistical analysis of quadratic response* surface model for reduction of aflatoxins by a cold plasma system.

Source	Sum of squares	Df	Mean square	*F*-value	*P* value
Model	3499.33	12	291.61	125.83	<0.0001
A-Q	1666.99	1	1666.99	719.32	<0.0001
B-Ar	17.40	1	17.40	7.51	0.0160
C-Tw	617.27	1	617.27	266.36	<0.0001
D-dos	215.22	1	215.22	92.87	<0.0001
AB	16.04	1	16.04	6.92	0.0198
AC	14.04	1	14.04	6.06	0.0274
AD	11.97	1	11.97	5.17	0.0393
BD	8.21	1	8.21	3.54	0.0808
CD	189.75	1	189.75	81.88	<0.0001
A^2	65.18	1	65.18	28.13	0.0001
B^2	499.42	1	499.42	215.50	<0.0001
D^2	11.81	1	11.81	5.10	0.0405
Residual	32.44	14	2.32		
Lack of fit	27.83	12	2.32	1.00	0.6021
Pure error	4.62	2	2.31		
Cor total	3531.78	26			

oxygen, superoxide anions, and ozone. RNS mainly includes nitrate, nitrite, peroxynitrite, nitric oxide radical (•NO), ammonia (NH_3), and nitrogen [26]. The long-lived reactive species are hydrogen peroxide, nitrate, and nitrite [27].

To prepare the simulation conditions of PAW, first, the structures of several reactive radical species existing in PAW, such as nitrate (NO_3^-), hydrogen peroxide (H_2O_2), and singlet oxygen ($^1O_2$), were retrieved from the PubChem website codes 943, 784, and 977 in SDF format, respectively. Due to the absence of the three-dimensional (3D) structure of the mentioned compounds on the PubChem website, the 3D structure was drawn using Chem 3D 18.0. Moreover, the tertiary structure of aflatoxins with code 14403 was retrieved from PubChem.

The compound minimization was done using UCSF Chimera software version 1.13 to minimize the energy of desired compounds before simulation, and the output of each file was saved in .pdb format. For the input file of the GROMACS software simulation to be prepared, first, it was necessary to prepare the initial file containing the given radicals with a specific concentration in an aqueous environment to establish PAW conditions in the presence of aflatoxins.

To this purpose, Packmol software (portable version) was used, and each of the three studied free radicals with the optimal state concentrations obtained using RSM for H_2O_2, $^1O_2$, and NO_3^- were placed in a box of water and aflatoxins and the output of each file was saved in .pdb format. Concentrations were obtained from PAW decomposition in the experimental laboratory. Next, three files related to the abovementioned free radicals were simulated separately. The MD simulation was performed with the GROMACS version 5.1.4.

As the target structures of this study have none of the four structures of proteins, nucleic acids, lipids, and sugars recognizable by GROMACS, the structures were prepared through the Acpype server (https://www.bio2byte.be/acpype) to create topology files. Moreover, the AMBER force field was selected in the GROMACS simulation for more accurate calculations. Then, each structure 3D file was introduced to GROMACS. The GROMACS Editconf command was used to create a .gro coordinate file. The simulation duration was defined as 25 nanoseconds (25,000 picoseconds) in the implementation of the simulation. Calculations related to the output of the data obtained from GROMACS were analyzed using Microsoft Excel 2016. The results are presented in graphs and tables with mean ± SD values.

4. Results and Discussion

4.1. Effect of PAW Application on Aflatoxin Control and Removal. Analysis of variance (ANOVA) was performed using stepwise regression and Box-Behnken design in Design-Expert 12 software. Table 2 shows the ANOVA results of the main and mutual effects of water flow under the influence of CAP, air/gas mixture (air + argon) ratio, PAW application time, and dose of the inoculated toxin on the reduction of aflatoxins in almonds. The results of the statistical analysis showed that all the parameters examined in this study, except the air/gas mixture (air + argon) ratio × PAW application time (BC) and squared PAW application time (C^2), are significant at the level of 10%. The nonsignificance of lack of fit, coefficient of determination (R^2) of 0.99, and standard error (std. dev) of 1.52 indicate an acceptable match between the experimental data and the simulated data obtained by the software, showing the sufficient accuracy of the model. The coded equation (2) was obtained based on the experimental results:

$$\begin{aligned} \mathrm{AFT} = {} & +31.91 - 11.79A + 1.20B + 7.17C + 4.24D \\ & + 2.00AB - 1.87AC - 1.73AD + 1.43BD \\ & + 6.89CD + 3.30A^2 - 9.12B^2 + 1.40D^2. \end{aligned} \quad (2)$$

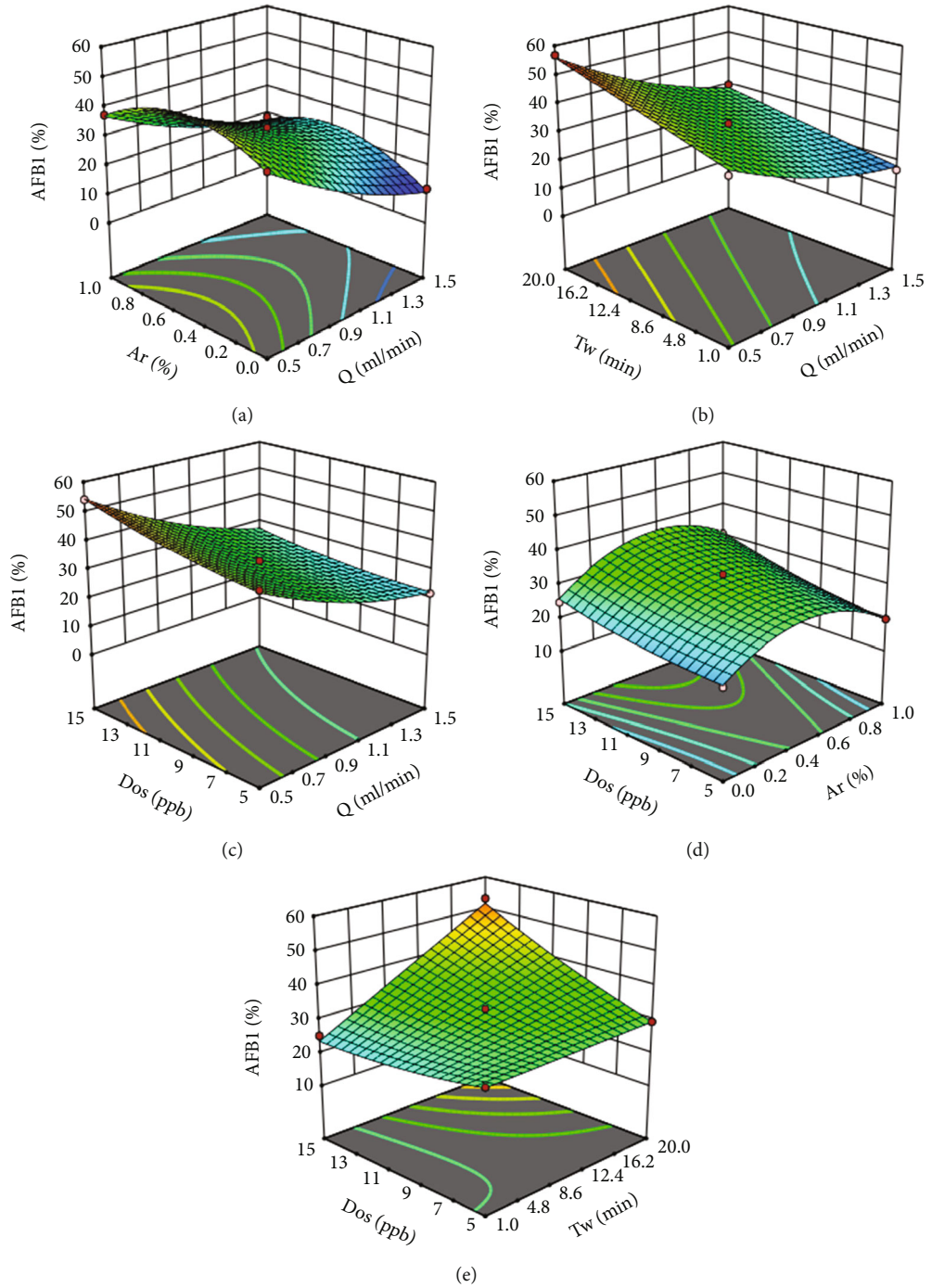

Figure 2: Percentage reduction of aflatoxins (a) 3D diagram of air/argon mixture ratio and PAW flow rate, (b) 3D diagram of PAW flow rate and the activated water application time, (c) 3D diagram of PAW flow rate and dose of inoculated toxin, (d) 3D diagram of air/argon mixture ratio and dose of inoculated toxin, and (e) 3D diagram of PAW application time and dose of inoculated toxin.

In the coded equation (2), the numerical values of the coefficients show the importance of each parameter such that the negative sign of the coefficient indicates the inverse effect and positive coefficients show the synergistic effect. Therefore, considering the numerical values of the coefficients, the flow rate of PAW (A) has the greatest effect on the reduction of almond aflatoxin B1, and the PAW application time (C), the dose of inoculated toxin (D), and air/gas mixture ratio (air + argon) (B) come next.

Figure 2(a) shows the 3D diagram of the effect of the PAW rate and the air/gas mixture (air+ argon) ratio on reducing aflatoxins. The figure shows that the flow rate of PAW had the greatest effect on reducing aflatoxins. Reducing the water flow rate from 1 to 0.5 ml/min has caused a

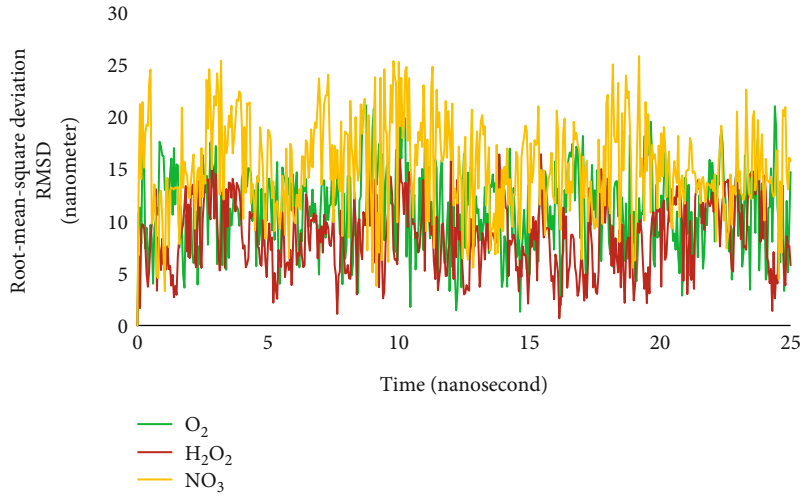

Figure 3: RMSD variation between aflatoxin and nitrate (NO_3^-), hydrogen peroxide (H_2O_2), and singlet oxygen ($^1O_2$) free radicals within 25 nanoseconds of MD simulation in water.

Table 3: Mean and standard deviation of RMSD and Rg (after 25 nanoseconds).

System	RMSD (nm)			Rg (nm)
	Aflatoxin-radical	Aflatoxin-water	Aflatoxin-aflatoxin	
O_2	3.9 ± 11.11	11.81 ± 2.06	0.029 ± 0.008	0.34 ± 0.003
H_2O_2	8.61 ± 3.46	4.18 ± 1.79	0.030 ± 0.009	0.34 ± 0.002
NO_3^-	15.10 ± 4.53	12.64 ± 2.55	0.029 ± 0.006	0.34 ± 0.002

greater reduction in aflatoxin concentration in the samples (the amount of aflatoxin B1 reduction in the flow rate of 0.5 ml/min has been reported to be 23% more than that of the flow rate of 1 ml/min). Moreover, by reducing the flow rate from 1.5 ml/min to 1 ml/min, the rate of aflatoxin B1 reduction has increased by 6.5%.

Figure 2(b) shows the 3D diagram of the effect of the PAW rate and the PAW activation time on reducing aflatoxins. This figure shows that the flow rate of PAW had the greatest effect on reducing aflatoxins compared with the PAW activation time. Reducing the water flow rate from 1.5 to 0.5 ml/min has caused an increase in the aflatoxin concentration reduction by 40%. Moreover, increasing the PAW application time from 1 to 10 and 10 to 20 minutes caused an increase in aflatoxin reduction by 7.17% and 7.15, respectively.

As the plasma application to water is prolonged, free radicals, positive and negative ions, and highly reactive ROS and RNS species generated and penetrated the water are increased. With the increase of these highly reactive species, water's reduction potential and oxidizing properties increase, and the environment's acidity increases as the pH decreases. Treating aflatoxin-contaminated almond samples with PAW destroys the aflatoxin structure and reduces its concentration.

The more time PAW is applied to samples, the greater the opportunity provided to the ions and free radicals to react and destroy the toxin. Such is a greater opportunity for free radicals to oxidize structures and affect aflatoxin particles. For this reason, by increasing the time of PAW application to samples, aflatoxins are better controlled and reduced.

Figures 2(c) and 2(d) show that the increased dose of aflatoxins inoculated to samples at the beginning of the experiment causes an increase in the toxin removal such that by increasing the initial dose from 5 ppb to 15 ppb, much more aflatoxins are reduced. By increasing the dose of inoculated toxin from 5 ppb to 10 ppb, the level of aflatoxin reduction has increased by 2.83%, and this level of toxin reduction reaches 5.63% when the dose of inoculated toxin increases from 10 ppb to 15 ppb.

Figure 2(e) shows the downward slope of the air/gas mixture (air + argon) ratio compared to the dose of the inoculated toxin. Considering the coefficients of equation (2), the dose of the inoculated toxin was found to have the greatest effect on reducing aflatoxins compared with the air/gas mixture (air + argon) ratio. Figure 2(e) shows that an increase in the air/gas (air + argon) ratio from 0 to 50% increased aflatoxin reduction by 9.3%, but an increase to 100% decreased by 6.93%. Due to CAP generation with air and argon sources, very reactive species of RNS and ROS have been produced, leading to complicated reactions in reaction to water level or by penetrating it. One of the most important reasons why plasma formed by different gases affects aflatoxins is the formation of free radicals and highly reactive species and their dissolution and penetration in PAW.

The more free radicals and reactive species in the PAW, the greater the destruction effect is on bacteria, viruses, and

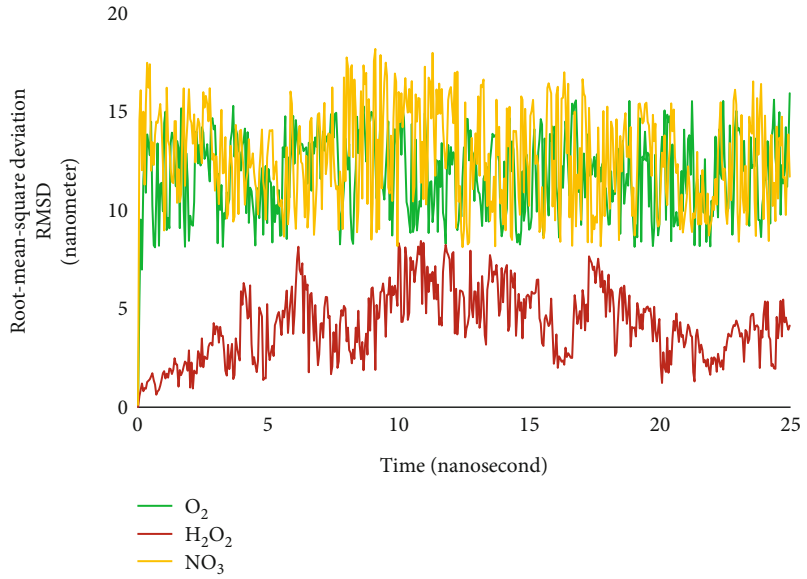

Figure 4: RMSD variation between aflatoxin and water within 25 nanoseconds of MD simulation in the presence of free radicals.

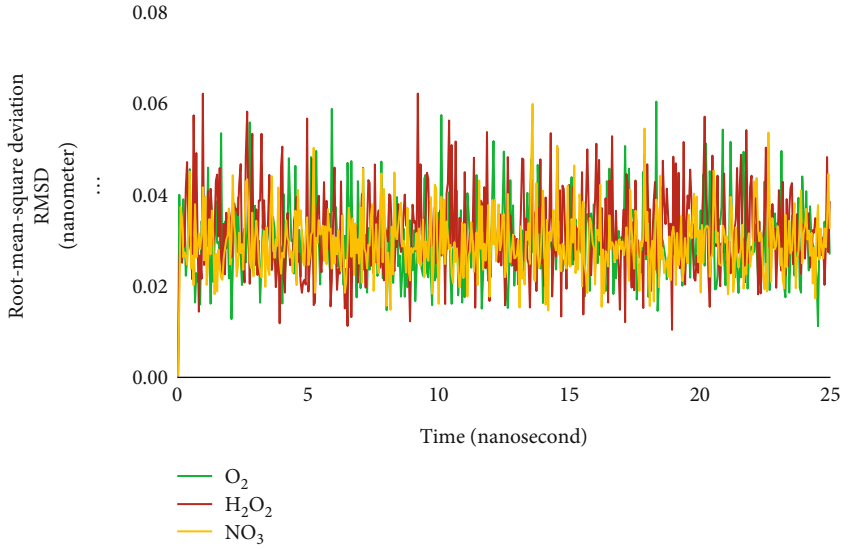

Figure 5: Interparticle variation of aflatoxin during MD simulation in the presence of PAW.

toxins in samples. Depending on the type of the utilized gas, the produced free radicals by applying the PAW are of different concentrations such that much more singlet oxygen ($^1O_2$), nitrogen monoxide (NO), nitrate (NO_3^-), and nitrite (NO_2^-) free radicals are generated in air-PAW than in argon-PAW [28, 29]. Additionally, more positive singlet hydrogen, hydroxyl, and hydrogen peroxide free radicals are found in argon-PAW compared to air-PAW [28, 29]. Therefore, the proper mixture of air and argon as the source of plasma generation is more efficient in reducing aflatoxins compared to the single use of each of them such that by combining these two gases, proper concentrations of RNSs and ROSs penetrate the PAW and destroy the structure of aflatoxins as are applied to the samples, this way control the toxin in samples.

4.2. Optimization. The results of optimizing the RSM for the highest reduction of aflatoxins are presented in Figure 3. The optimal values for water flow rate, percentage of argon gas and air mixture, PAW application time, and dose of the inoculated toxin in the designed system were found to be 0.5 ml/min, 86% argon gas, 17.71 min, and 14.7 ppb, respectively. The obtained values led to a 61.6636% reduction in aflatoxins. To validate the optimized points, the level of aflatoxin reduction was tested on a laboratory scale, and the reduction level was found to be 62%. This minor difference between the theoretical optimal value and the laboratory result indicates the precision of the optimization method.

4.3. Results of MD Simulation and In Silico Laboratory. The optimal conditions obtained from the experiments were

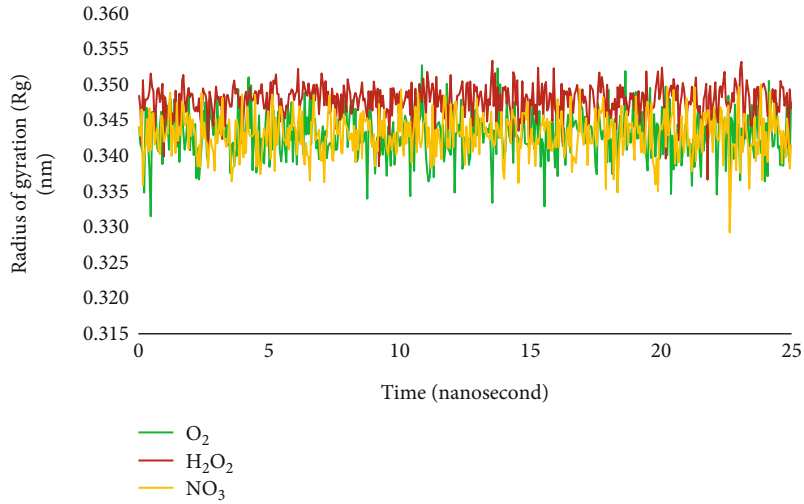

Figure 6: The radius of gyration (Rg) of aflatoxin during MD simulation in the presence of PAW.

Table 4: The mean number of hydrogen bonds between aflatoxin B1 water and the dissolution of aflatoxin B1 in the presence of free radicals (after 25 nanoseconds).

System	Hydrogen bonding between water (solvent) and aflatoxin
O_2	3.42 ± 1.36
H_2O_2	3.36 ± 1.36
NO_3^-	3.42 ± 1.38

Table 5: Free energy of total binding between aflatoxin and free radicals.

System	ΔG bind
O_2	(i) 2.73 ± 0.56
H_2O_2	(ii) 58.31 ± 8.36
NO_3^-	(iii) 2.73 ± 8.36

utilized to investigate the impact of PAW on the structure of aflatoxin B1. The concentration of three target free radicals (H_2O_2, $^1O_2$, and NO_3^-) was measured using the PAW generation system (Figure 2) under the optimal conditions (86% argon and water flow rate of 0.5 ml/min). The concentrations of H_2O_2, $^1O_2$, and NO_3^- were found to be approximately 4 ppm, 21 ppm, and 5 ppm, respectively. Free radicals were then placed in a box containing water and aflatoxin B1 at the aforementioned concentrations, and a simulation of PAW containing nitrate (NO_3^-), hydrogen peroxide (H_2O_2), and singlet oxygen ($^1O_2$) free radicals was conducted in the presence of aflatoxin B1 for 25 nanoseconds.

Figure 3 depicts the RMSD variations between aflatoxin B1 and free radicals within 25 nanoseconds of MD simulation in water. The figure reveals that H_2O_2 exhibited a weaker performance compared to the other two free radicals. Furthermore, NO_3^- displayed more effective performance due to the higher level of the diagram, indicating that NO_3^- caused destruction and instability of the aflatoxin B1 structure and destroyed the aflatoxin B1 more effectively than the other studied radicals.

As shown in Table 3, the RMSD variation between aflatoxin B1 and free radicals is the least effective for H_2O_2 (mean = 8.61 ± 3.46 nm) compared to the other two free radicals.

Regarding the RMSD variation between aflatoxin B1 and water in the presence of free radicals, Table 3 shows H_2O_2 with a mean of 4.81 ± 1.79 (nm) and NO_3^- with a mean of 12.64 ± 2.55 (nm) has the most and least effect on the aflatoxin B1 structure, respectively. Figure 4 also clearly shows the significantly different performance of H_2O_2 compared to the other two free radicals.

Figure 5 also shows the interparticle variation of aflatoxin B1 during MD simulation in the presence of PAW. The data in Table 3 shows no significant difference between the three studied free radicals.

As shown in Table 3, the radius of gyration (Rg) of aflatoxin B1 variation during MD simulation in the presence of the PAW indicated that the three species mentioned above have a numerical variation of 0.34 ± 0.002. This variation process can also be seen in Figure 6.

Regarding the mean number of hydrogen bonds between water and aflatoxin B1 and according to the data (Table 4), H_2O_2 was found to have a numerical mean of 3.36 ± 1.36. Moreover, NO_3^- and O_2 free radicals show no significant difference in forming hydrogen bonds and have almost the same performance. These two species have the same interactions with solvent and water molecules.

The total binding free energy (Digibind, kcal/mol) is estimated using the software as follows:

$$\Delta G\,\text{bind} = G\,\text{complex} - (G\,\text{aflatoxin} + G\,\text{radical}). \quad (3)$$

According to Table 5, the bond energy between H_2O_2 and aflatoxin B1 with a numerical value of −58.31 ± 8.36 is the most appropriate value, and O_2 with the mean value of −2.73 ± 0.56 is the least value of ΔG.

Table 6: Amount of total energy, potential energy, kinetic energy, enthalpy, temperature, and density during simulation.

	O_2	H_2O_2	NO_3^-
Potential energy (kJ/mol)	−2081622 ± 8322.21	−1040151.57 ± 4298.64	−20811755.50 ± 8314.12
Kinetic energy (kJ/mol)	374239.67 ± 1035.88	187298.99 ± 1131.95	374256.40 ± 1049.21
Total energy (kJ/mol)	−1707382.52 ± 8364.07	−852852.57 ± 4570.96	−1706919.09 ± 839.25
Density (kg/m^3)	976.28 ± 1.63	976.78 ± 2.03	976.27 ± 1.62
Enthalpy (kJ/mol)	−1707290 ± 8365.076	−1856616.18 ± 194661.10	−1706826.79 ± 8392.34
Temperature (K)	299.99 ± 0.83	300.19 ± 1.81	300.00 ± 0.84

Table 6 shows the mean value of energy during the 25 nanoseconds simulation, mean kinetic energy, total energy over time, mean temperature, density, and mean enthalpy for aflatoxin B1 in the presence of PAW and studied free radicals.

According to the MD simulation, the results can be interpreted as follows:

The RMSD factor is a commonly used metric for assessing the variations in the tertiary structure of compounds and proteins during the simulation process. Additionally, it can indicate whether the protein is charged or not. Thus, an increase in RMSD in the presence of factors that affect a compound suggests increased stability of the compound in the presence of those factors [30]. The results of the present study demonstrate that the NO_3^- free radical increases the RMSD value more than O_2 and H_2O_2, suggesting that NO_3^- can more effectively reduce the activity level of aflatoxin B1 and further inhibit its function by increasing interatomic movements compared to the other two reactive species.

Furthermore, the mean variation of RMSD in the aflatoxin B1-free radical complex in the presence of H_2O_2, O_2, and NO_3^- is presented in Figure 4 and Table 3. The analysis reveals that the reduction of RMSD value is greater in the presence of H_2O_2, and the variation fluctuation is less. This suggests that the inhibition rate of aflatoxin B1 is lower in the presence of H_2O_2 than in the presence of the other two free radicals.

The radius of gyration (Rg) of a protein complex measures its compactness. A stable compound maintains a consistent Rg value, while an unstable compound that is subject to unfolding or breaking will exhibit an increase in Rg value during simulation [31]. Generally, the smaller the Rg, the more compact the given compound, and the higher the probability of its thermal stability [32]. According to Figure 6 and data related to the Rg level shown in Table 3, it is clear that aflatoxin B1 has the same level of access to three free radicals, and therefore, the probability of its thermal stability in the presence of all three reactive species is almost equal.

Based on the mean number of hydrogen bonds between PAW and aflatoxin B1 presented in Table 4, it can be concluded that aflatoxin B1 exhibits fewer hydrogen bonds with water molecules in the presence of H_2O_2, indicating that this reactive species of free radicals induces fewer changes in the solubility of aflatoxin B1 and encourages the compound to adopt a more stable structure. Typically, an increase in the number of hydrogen bonds strengthens this bond beyond the van der Waals interaction energy, increasing compound solubility if the number of hydrogen bonds increases [33].

Table 5 indicates that the binding energy between aflatoxin B1 and free radicals is most appropriate for H_2O_2 with a ΔG bind value. Therefore, it is reasonable to suggest that NO_3^- can have a more pronounced impact on aflatoxin B1 by establishing a stronger connection with the compound and ultimately influencing its activity or causing its destruction. As shown in Table 6, the potential energy during the 25-nanosecond simulation reveals that all three free radical species, particularly NO_3^-, can significantly increase the system's energy level in the presence of aflatoxin B1, thereby affecting it. The reduction in temperature during the simulation of aflatoxin B1 in the presence of O_2 (Table 6) suggests that the effect of this reactive species on aflatoxin B1 is less than that of the other two species. In general, the MD parameters demonstrate that the free radicals examined in the PAW framework can affect the structure of aflatoxin B1 and alter it.

5. Conclusion

The results of using PAW for aflatoxin control and removal indicate that a reduction in the flow rate of plasma-treated water has the most significant impact on reducing aflatoxins, followed by PAW application time, the dose of inoculated toxin, and the air/argon mixture (air + argon) ratio. Various treatments were conducted to evaluate the effect of PAW on aflatoxins, resulting in a reduction of 12% to 56.8% in almonds. Optimal values for the water flow rate, percentage of argon gas and air mixture, PAW application time, and dose of the inoculated toxin were determined to be 0.5 ml/min, 86% argon gas, 17.71 min, and 14.7 ppb, respectively. MD simulation was employed to assess the effect of PAW on aflatoxin B1. MD is a computer simulation method that analyzes the physical movements of atoms and molecules, providing insight into the dynamic "evolution" of the system. The effect of PAW under the influence of the active species of nitrate (NO_3^-), hydrogen peroxide (H_2O_2), and singlet oxygen ($^1O_2$) free radicals on aflatoxin B1 inhibition or form changes were evaluated. The results indicate that the average RMSD variation between aflatoxin B1 and free radicals was 8.61 ± 3.46 for H_2O_2. Additionally, the variation in the radius of gyration (Rg) of aflatoxin B1 was equal to 0.34 ± 0.002 for all three radical active species, and the mean number of hydrogen bonds between water and aflatoxin B1 was 3.36 ± 1.36 for H_2O_2. Overall, the findings demonstrate that the use of PAW can alter the structure of aflatoxin B1, ultimately reducing its toxicity by changing and inhibiting its activity.

Data Availability

The data used to support the findings of this study are included in the article.

Conflicts of Interest

The authors do not have any conflicts of interest.

Acknowledgments

The Research Council of Shahrekord University is thankfully acknowledged for the financial support to carry out the work (grant no.: 97GRN31M1007).

References

[1] N. E. Caicedo Solano, G. A. García Llinás, and J. R. Montoya-Torres, "Towards the integration of lean principles and optimization for agricultural production systems: a conceptual review proposition," *Journal of the Science of Food and Agriculture*, vol. 100, no. 2, pp. 453–464, 2020.

[2] B. C. Campbell, R. J. Molyneux, and T. F. Schatzki, "Current research on reducing Pre- and post-harvest aflatoxin contamination of U.S. almond, pistachio, and walnut," *Journal of Toxicology: Toxin Reviews*, vol. 22, no. 2-3, pp. 225–266, 2003.

[3] D. Guo, H. Liu, L. Zhou, J. Xie, and C. He, "Plasma-activated water production and its application in agriculture," *Journal of the Science of Food and Agriculture*, vol. 101, no. 12, pp. 4891–4899, 2021.

[4] T. Iqbal, M. Farooq, S. Afsheen, M. Abrar, M. Yousaf, and M. Ijaz, "Cold plasma treatment and laser irradiation ofTriticumspp. seeds for sterilization and germination," *Journal of Laser Applications*, vol. 31, no. 4, article 042013, 2019.

[5] J.-W. Kim, P. Puligundla, and C. Mok, "Microbial decontamination of dried laver using corona discharge plasma jet (CDPJ)," *Journal of Food Engineering*, vol. 161, pp. 24–32, 2015.

[6] L. Li, J. Li, H. Shao, and Y. Dong, "Effects of low-vacuum helium cold plasma treatment on seed germination, plant growth and yield of oilseed rape," *Plasma Science and Technology*, vol. 20, no. 9, article 095502, 2018.

[7] D. Liu, Z. C. Liu, C. Chen et al., "Aqueous reactive species induced by a surface air discharge: heterogeneous mass transfer and liquid chemistry pathways," *Scientific Reports*, vol. 6, no. 1, article 23737, 2016.

[8] S. Amaike and N. P. Keller, "Aspergillus flavus," *Annual Review of Phytopathology*, vol. 49, no. 1, pp. 107–133, 2011.

[9] N. N. Misra, B. K. Tiwari, K. S. M. S. Raghavarao, and P. J. Cullen, "Nonthermal plasma inactivation of food-borne pathogens," *Food Engineering Reviews*, vol. 3, no. 3-4, pp. 159–170, 2011.

[10] N. N. Misra, B. Yadav, M. S. Roopesh, and C. Jo, "Cold plasma for effective fungal and mycotoxin control in foods: mechanisms, inactivation effects, and applications," *Comprehensive Reviews in Food Science and Food Safety*, vol. 18, no. 1, pp. 106–120, 2019.

[11] A. Patange, P. Lu, D. Boehm, P. J. Cullen, and P. Bourke, "Efficacy of cold plasma functionalised water for improving microbiological safety of fresh produce and wash water recycling," *Food Microbiology*, vol. 84, article 103226, 2019.

[12] S. Samukawa, M. Hori, S. Rauf et al., "The 2012 plasma roadmap," *Journal of Physics D: Applied Physics*, vol. 45, no. 25, article 253001, 2012.

[13] B. Adhikari, M. Adhikari, B. Ghimire, G. Park, and E. H. Choi, "Cold atmospheric plasma-activated water irrigation induces defense hormone and gene expression in tomato seedlings," *Scientific Reports*, vol. 9, no. 1, article 16080, 2019.

[14] J. C. Fountain, B. T. Scully, X. Ni et al., "Environmental influences on maize-*Aspergillus flavus* interactions and aflatoxin production," *Frontiers in Microbiology*, vol. 5, p. 40, 2014.

[15] G. Kamgang-Youbi, J. M. Herry, T. Meylheuc et al., "Microbial inactivation using plasma-activated water obtained by gliding electric discharges," *Letters in Applied Microbiology*, vol. 48, no. 1, pp. 13–18, 2009.

[16] R. Ma, G. Wang, Y. Tian, K. Wang, J. Zhang, and J. Fang, "Nonthermal plasma-activated water inactivation of food-borne pathogen on fresh produce," *Journal of Hazardous Materials*, vol. 300, pp. 643–651, 2015.

[17] E. Tsoukou, P. Bourke, and D. Boehm, "Understanding the differences between antimicrobial and cytotoxic properties of plasma activated liquids," *Plasma Medicine*, vol. 8, no. 3, pp. 299–320, 2018.

[18] M. Ma, Y. Zhang, Y. Lv, and F. Sun, "The key reactive species in the bactericidal process of plasma activated water," *Journal of Physics D: Applied Physics*, vol. 53, no. 18, p. 185207, 2020.

[19] B. G. Dasan, I. H. Boyaci, and M. Mutlu, "Inactivation of aflatoxigenic fungi (Aspergillus spp.) on granular food model, maize, in an atmospheric pressure fluidized bed plasma system," *Food Control*, vol. 70, pp. 1–8, 2016.

[20] J. Yu, "Current understanding on aflatoxin biosynthesis and future perspective in reducing aflatoxin contamination," *Toxins*, vol. 4, no. 11, pp. 1024–1057, 2012.

[21] X. Guo, Y. Liu, and J. Wang, "Sorption of sulfamethazine onto different types of microplastics: a combined experimental and molecular dynamics simulation study," *Marine Pollution Bulletin*, vol. 145, pp. 547–554, 2019.

[22] M. Zarringhalam, H. Ahmadi-Danesh-Ashtiani, D. Toghraie, and R. Fazaeli, "Molecular dynamic simulation to study the effects of roughness elements with cone geometry on the boiling flow inside a microchannel," *International Journal of Heat and Mass Transfer*, vol. 141, pp. 1–8, 2019.

[23] X. Kong, "Pattern mining and visualization for molecular dynamics," *Bioinformatics*, vol. 12, p. 445, 2011.

[24] Z. Esmaeili, B. Hosseinzadeh Samani, F. Nazari, S. Rostami, and A. Nemati, "The green technology of cold plasma jet on the inactivation ofAspergillus flavusand the total aflatoxin level in pistachio and its quality properties," *Journal of Food Process Engineering*, vol. 46, no. 1, article e14189, 2023.

[25] B. Hosseinzadeh Samani, A. Behruzian, M. H. Khoshtaghaza, M. Behruzian, and A. Ansari Ardali, "The investigation and optimization of two combined pasteurization methods of ultrasonic-pulse electric field and hydrodynamic-pulse electric field on sour cherry juice using RSM-TOPSIS," *Journal of Food Processing and Preservation*, vol. 44, no. 9, Article ID e14700, 2020.

[26] R. Thirumdas, A. Kothakota, U. Annapure et al., "Plasma activated water (PAW): chemistry, physico-chemical properties, applications in food and agriculture," *Trends in Food Science & Technology*, vol. 77, pp. 21–31, 2018.

[27] N. K. Kaushik, B. Ghimire, Y. Li et al., "Biological and medical applications of plasma-activated media, water and solutions," *Biological Chemistry*, vol. 400, no. 1, pp. 39–62, 2019.

[28] T. Takamatsu, K. Uehara, Y. Sasaki et al., "Microbial inactivation in the liquid phase induced by multigas plasma jet," *PLoS One*, vol. 10, no. 7, article e0132381, 2015.

[29] T. Takamatsu, A. Kawate, K. Uehara et al., "Bacterial inactivation in liquids using multi-gas plasmas," *Plasma Medicine*, vol. 2, no. 4, pp. 237–247, 2012.

[30] Q. Wu, L. Zhou, X. Sun et al., "Altered lipid metabolism in recovered SARS patients twelve years after infection," *Scientific Reports*, vol. 7, no. 1, p. 9110, 2017.

[31] R. T. McGibbon, K. A. Beauchamp, M. P. Harrigan et al., "MDTraj: a modern open library for the analysis of molecular dynamics trajectories," *Biophysical Journal*, vol. 109, no. 8, pp. 1528–1532, 2015.

[32] A. S. Bhat, R. Dustin Schaeffer, L. Kinch, K. E. Medvedev, and N. V. Grishin, "Recent advances suggest increased influence of selective pressure in allostery," *Current Opinion in Structural Biology*, vol. 62, pp. 183–188, 2020.

[33] C. G. P. Doss, B. Rajith, N. Garwasis et al., "Screening of mutations affecting protein stability and dynamics of FGFR1—a simulation analysis," *Applied & Translational Genomics*, vol. 1, pp. 37–43, 2012.